Tree Physiology 37, 815–826
doi:10.1093/treephys/tpx022

Research paper

Surface properties and physiology of *Ulmus laevis* and *U. minor* samaras: implications for seed development and dispersal

Paula Guzmán-Delgado[1,2,4], Victoria Fernández[1], Martin Venturas[1,3], Jesús Rodríguez-Calcerrada[1] and Luis Gil[1]

[1]Forest Genetics and Ecophysiology Research Group, School of Forest Engineering, Technical University of Madrid, Ciudad Universitaria, Madrid 28040, Spain; [2]Present address: Department of Plant Sciences, University of California Davis, One Shields Avenue, Davis, CA 95616, USA; [3]Present address: Department of Biology, University of Utah, 257 South 1400 East, Salt Lake City, UT 84112, USA; [4]Corresponding author (pguzmandelgado@ucdavis.edu)

Received August 11, 2016; accepted February 28, 2017; published online March 21, 2017; handling Editor Ülo Niinemets

Plant surface properties influence solid–liquid interactions and matter exchange between the organs and their surrounding environment. In the case of fruits, surface processes may be of relevance for seed production and dispersal. To gain insight into the relationship between surface structure, chemical composition and function of aerial reproductive organs, we performed diverse experiments with the dry, winged fruits, or samaras, of *Ulmus laevis* Pall. and *Ulmus minor* Mill. both at the time of full maturity (green samaras) and of samara dispersal (dry samaras). Samaras of both elm species showed positive photosynthetic rates and absorbed water through their epidermal surfaces. The surface wettability, free energy, polarity and solubility parameter were lower in *U. laevis* than in *U. minor* and decreased for dry samaras in both species. *Ulmus laevis* samaras had a high degree of surface nano-roughness mainly conferred by cell wall folds containing pectins that substantially increased after hydration. The samaras in this species also had a thicker cuticle that could be isolated by enzymatic digestion, whereas that of *U. minor* samaras had higher amounts of soluble lipids. Dry samaras of *U. laevis* had higher floatability and lower air sustentation than those of *U. minor*. We concluded that samaras contribute to seed development by participating in carbon and water exchange. This may be especially important for *U. minor*, whose samaras develop before leaf emergence. The trichomes present along *U. laevis* samara margin may enhance water absorption and samara floatability even in turbulent waters. In general, *U. minor* samaras show traits that are consistent with a more drought tolerant character than *U. laevis* samaras, in line with the resources available both at the tree and ecosystem level for these species. Samara features may additionally reflect different adaptive strategies for seed dispersal and niche differentiation between species, by favoring hydrochory for *U. laevis* and anemochory for *U. minor*.

Keywords: cell wall, cuticle, pectins, plant surfaces, seed dispersal, water interactions.

Introduction

The epidermis of primary aerial organs of plants plays a major role in the regulation of matter exchange with the atmosphere (Riederer and Schreiber 2001, Zwieniecki and Boyce 2014). Among epidermal structures, the cuticle is commonly considered a fixed barrier to transpirational water loss, which would make gas exchange dynamically controlled by stomata (Yeats and Rose 2013). The contribution of the cuticle and stomata to liquid water absorption remains under debate (Fernández and Eichert 2009, Burkhardt et al. 2012). In general, the mechanisms underlying the transport of substances (e.g., water, CO_2) across the epidermal surface remain unknown (Damour et al. 2010, Guzmán et al. 2014*a*, 2014*b*, Boyer 2015, Buckley 2016).

The analysis of plant surface structure and chemical composition, and of the physico-chemical properties derived (Holloway 1970, Khayet and Fernández 2012) can provide information on the interactions between molecules that cross the surface and

the surface itself. Further physiological and ecophysiological interpretations can be inferred, as shown for liquid water and leaf surfaces (e.g., Brewer and Smith 1994, 1997, Andolfillo et al. 2002, Hanba et al. 2004, Aryal and Neuner 2010, van Wittenberghe et al. 2012, Fernández et al. 2014*b*, Goldsmith et al. 2016). Nevertheless, the significance of plant surface–water interactions and, in general, solid–liquid interactions, is unclear (Pierce et al. 2001, Rosado and Holder 2013), as is the physical basis for such interfacial phenomena (Kwok and Neumann 1999, Fernández and Khayet 2015).

Similar to plant surface–water interactions, the quantification, analysis and ecological interpretation of carbon and water exchange have mostly been conducted in leaves (e.g., Farquhar et al. 1989, Fernández and Eichert 2009). In this regard, some studies revealed that foliar absorption of surface-deposited water can improve plant water status (e.g., Boucher et al. 1995, Gouvra and Grammatikopoulos 2003, Breshears et al. 2008, Berry et al. 2014, Fernández et al. 2014*b*, Eller et al. 2016), and also influence net photosynthetic CO_2 uptake (Smith and McClean 1989, Munné-Bosch et al. 1999, Simonin et al. 2009). Although green leaves are the main sources of photosynthate production, other plant organs such as green fruits can display positive rates of atmospheric CO_2 uptake during part of their life-span and contribute to their own carbohydrate requirements for growth and maintenance (Aschan and Pfanz 2003). Fruit production and seed dispersal are key stages of a plant's life cycle that determine processes such as colonization of new habitats, maintenance of diversity, seedling establishment and population structure (Nathan and Muller-Landau 2000, Wang and Smith 2002). Thus, understanding carbon and water balance during fruit production and the role of fruit characteristics involved in seed dispersal is important to fully comprehend the ecology of species.

Samaras are dry indehiscent winged fruits that are dispersed by wind (anemochory) or water (hydrochory; Willson and Traveset 2000). Among other functions, the wings and hairs of fruits have been proposed to facilitate sustentation and floatability for their dispersal (Seiwa et al. 2008, Nilsson et al. 2010). Moreover, the samara wings of some species have been reported to exhibit positive rates of net photosynthetic CO_2 uptake (P_n) before they dry out and disperse; this is the case for green maple (*Acer platanoides*, Aschan and Pfanz 2003), and for some dipterocarp species (Kenzo et al. 2003). However, there is no information about the physico-chemical properties of samara wings and their role in physiological processes (mainly water and gas exchange), or their dispersal.

Ulmus laevis Pall. (European white elm) and *Ulmus minor* Mill. (field elm) are two deciduous tree species mainly distributed across southern and central Europe. Both elm species produce bulk quantities of samaras that remain green on the trees before they dry and disperse. However, *U. minor* samaras develop in late winter–early spring, several weeks before shoots flush, while *U. laevis* phenology is more delayed and its samaras develop in spring almost simultaneously with leaf appearance (Figure 1). In addition, *U. minor* samaras are subsessile (i.e., with short pedicels), whereas *U. laevis* samaras have long, articulated pedicels and ciliated margins (Figure 1), these characteristics being some of the main morphological differences between the two elm clades to which each species belongs (Wiegrefe et al. 1994). *Ulmus laevis* populations are chiefly found in riverbeds and seasonally waterlogged forests, whereas those of *U. minor* are in flood-plain forests linked to shallow water-tables (Venturas et al. 2014*a*). The niches each species occupy are associated, among other factors, with a higher susceptibility to drought (Venturas et al. 2013) and tolerance to flooding (Li et al. 2015) of *U. laevis* than *U. minor*. Elm samaras are dispersed by wind and water, and not by animals, which are seed predators (Perea et al. 2013, Venturas et al. 2014*b*).

The study of surface properties of *U. laevis* and *U. minor* samaras may provide insight into the environmental and ecological significance of these leafy fruits that reflect trait-based and phylogenetic differences between the species. We hypothesized that samaras can contribute to their self-maintenance by absorbing atmospheric water and exhibiting positive P_n. Their specific morpho-chemical characteristics may also favor hydrochory for *U. laevis* and anemochory for *U. minor*, and the occupancy of different niches by the species. By following an integrative approach, we aimed to address three questions: (i) do green (at full maturity) and dry (at their abscission and dispersal time) samaras of *U. laevis* and *U. minor* have similar surface structure, chemical composition and physico-chemical properties; (ii) can samaras contribute to seed water and carbon economy; and (iii) how can samara surface properties be interpreted in terms of facilitating samara dispersal and seedling establishment?

Materials and methods

Plant material

Fully developed, undamaged *U. laevis* and *U. minor* samaras (sometimes referred to as *U. laevis* and *U. minor* along the text)

Figure 1. Branches of *U. laevis* (A) and *U. minor* (B) with fully developed green samaras. The photographs are not at the same scale. Samara projected surface area is ~1 cm^2 for *U. laevis* and ~4 cm^2 for *U. minor*. Note the presence of expanding leaves in *U. laevis* vs closed vegetative buds in *U. minor*.

were selected for this study. Except for a sustentation experiment, samaras were located at the apex of external, east-facing shoots of six trees (three in the case of carbon exchange measurements) per species growing at 'Puerta de Hierro' nursery (Madrid, Spain; 40.45° N, 3.75° W) within a conservation plot of the Spanish Elm Breeding Program. For the sustentation trial, samaras at different positions around the crown of three trees per species were selected from the previous location in the case of *U. minor* and from Valdelatas forest (Madrid, Spain; 40.53° N, 3.68° W) in that of *U. laevis*.

Samaras were analyzed either attached to the trees or after detachment from shoots. Shoots were collected from branches kept in water for 15 min before laboratory measurements. The analyses were performed on samaras at approximately the time of full maturity (referred to as green samaras) and at the time of pedicel abscission (referred to as dry samaras), the latter being coincident with samara dispersal period.

The mean values of relative humidity (RH) and temperature at the 'Puerta de Hierro' location for the 8-day period prior to green samara analyses ranged from 89% to 13%, and 0.3–25.2 °C for *U. minor* and between 91% and 20%, and 4.7–22.1 °C for *U. laevis* (data collected from 'Madrid Puerta de Hierro' weather station, 1–13 April 2015). Since dew condensation on the samara surfaces was observed during early morning, higher RH and/or lower temperature values were expected to be reached at least at the experimental plots where the trees were located. Similar environmental conditions were recorded at the time of samara abscission (data not shown).

Determination of physico-chemical properties of samara surfaces

Thermodynamic approaches can be used to characterize the properties of solid surfaces, such as those of plants, in relation to liquid interactions. The measurement of drop contact angles (θ) deposited on to a surface is the most frequently used methodology to estimate the tendency of a plant surface to be wet, i.e., its wettability (Koch and Barthlott 2009). Intrinsic properties of a solid surface such as the surface free energy (γ) can be additionally determined by measuring θ of drops of liquids with different degrees of polarity (van Oss et al. 1987, 1988). Considering the type of molecular interactions occurring at the surface of a solid (s) (or liquid, l), the total surface free energy (γ_s) (or surface tension, γ_l) can be expressed as the sum of the Lifshitz-van der Waals (γ_s^{LW}, or dispersive component) and the acid–base (γ_s^{AB}, or non-dispersive component; Fowkes 1963, van Oss et al. 1987, 1988). While the γ is commonly used in artificial solid surface characterization, it has only recently been applied to intact plant surfaces (Fernández et al. 2011, Fernández and Khayet 2015). The solubility parameter (δ) as first introduced by Hildebrand (1949) and further developed by various researchers (e.g., van Krevelen and Hoftyzer 1976, Hansen 2004) enables the quantification of the cohesive properties of a substance and the degree of interaction between molecules (van Krevelen and te Nijenhuis 2009). While prediction of solubility parameters is commonly used, e.g., for the design and fabrication of polymeric membranes (Khayet et al. 2007), in the coating industry (Hansen 2004) or in pharmacology (Hancock et al. 1997), it was first applied by Khayet and Fernández (2012) to analyze the properties and potential thermodynamic interactions between plant surface chemical constituents and an array of agrochemicals. Although it can be predicted from molecular structures, the δ of a certain surface can also be derived after measuring contact angles of different liquids followed by the calculation of the total surface free energy and the cohesive energy density (Khayet and Fernández 2012).

To characterize the surface properties of green and dry samaras, advancing θ of drops of double-distilled water, glycerol and diiodomethane (the last two of 99% purity; Sigma-Aldrich, Munich, Germany) were measured on intact surfaces using a drop shape analyzer DSA100 (Krüss GmbH, Hamburg, Germany). Wing mid-sections of each samara side were cut with a scalpel and mounted on to microscope slides with double-sided adhesive tape. Two microliter drops of each liquid were deposited on to the surfaces with a manual dosing system holding a 1 ml syringe with a 0.5-mm-diameter needle (number of samples (n) = 30 per species, samara type and side). Contact angles were automatically calculated by fitting the captured drop shape to the one calculated from the Young-Laplace equation. Measurements were performed at room temperature (20 °C).

The total surface free energy (γ_s) and its components, i.e., the Lifshitz-van der Waals (γ_s^{LW}) and acid–base (γ_s^{AB}), the polarity ($\gamma_s^{AB}\gamma_s^{-1}$) and the total solubility parameter (δ) of the samara surfaces, were estimated (Fernández et al. 2011, Khayet and Fernández 2012). The surface tension of the liquids (γ_l) and its components (with γ_l^{AB} divided into the electron acceptor (γ^+) and electron donor (γ^-) interactions; van Oss et al. 1987) were: γ_l = 72.80 mJ m^{-2}, γ^{LW} = 21.80 mJ m^{-2}, $\gamma^+ = \gamma^-$ = 25.50 mJ m^{-2} for water; γ_l = 63.70 mJ m^{-2}, γ^{LW} = 30.10 mJ m^{-2}, γ^+ = 8.41 mJ m^{-2}, γ^- = 31.16 mJ m^{-2} for glycerol; and $\gamma_l = \gamma^{LW}$ = 50.80 mJ m^{-2}, γ^+ = 0.56 mJ m^{-2}, γ^- = 0 mJ m^{-2} for diiodomethane (Fernández and Khayet 2015).

Extraction and determination of soluble lipids

Soluble cuticular lipids (or waxes) were extracted by dipping intact green and dry samaras (n = 40 *U. minor*, and 60 *U. laevis*, 2 repetitions) into 150 ml of chloroform for 1 min. Extracts were evaporated until dryness, weighed and, in the case of green samaras, saved for gas chromatography coupled to mass spectrometry (GC–MS) analysis. The amount of soluble lipids was expressed on a dry weight (DW) basis.

For GC–MS, samples were filtered using PTFE filters prior to injection in a GC–MS apparatus (GC Varian CP-3800 coupled to a MS ion trap Varian Saturn 2200, GC-ITMS, automatic injector COMBI-PAL; CTC Analytics, Zwingen, Switzerland). The

chromatographic conditions were as follows (86 min per run): injection volume 1 µl, with helium as carrier gas (1.2 ml min^{-1}), and injector temperature 290 °C. The column (SLB-5 ms fused silica capillary column, 30 m × 0.25 mm × 0.25 µm film thickness; Supelco, Sigma-Aldrich) was set to 40 °C (3 min), heating rate of 10 °C min^{-1} up to 290 °C (18 min), and 20 °C min^{-1} up to 310 °C (13 min). The MS conditions were: 70 eV ionization voltage, 150 °C trap temperature, 20–550 units of mass scan range with 8 min solvent delay. The compounds were identified and quantified by comparing their mass spectra with NIST library spectra and analyzing the corresponding peaks of GC–MS ion chromatograms.

Enzymatic treatments

Green samaras, both intact and after soluble lipid extraction, were immersed in enzymatic solutions to evaluate the effect of enzyme hydrolysis on samara tissues. The solutions contained either 2% cellulase, 2% pectinase, or a mixture of 2% cellulase plus 2% pectinase (Novozymes, Bagsvared, Denmark), plus 1% PVP (Sigma-Aldrich) and 2 mM NaN_3. The pH was adjusted to 5.0 by adding sodium citrate (Guzmán et al. 2014*a*). A surfactant at 0.01% concentration (Break-Thru, Evonik Industries, Essen, Germany; γ_l ~22 mN m^{-1}) was also added to facilitate the hydrolysis process. Samaras were maintained in the solutions for 1 month at room temperature (19–21°C), carefully shaking the flasks at frequent time intervals. The effect of enzymes on *U. laevis* trichomes was assessed by subjecting samaras to digestion periods from 1 to 5 days (without surfactant). At the end of the various digestion periods, isolated cuticles and samaras of *U. laevis* (the cuticle of *U. minor* could not be successfully isolated) were selected, air-dried and stored for microscopic observation.

Microscopy

Gold-sputtered, intact (green and dry) and chloroform-extracted samaras of both species, as well as *U. laevis* enzymatically digested samaras and the upper and lower sides of the isolated cuticles were examined by scanning electron microscopy (SEM). A Philips XL30 SEM (Eindhoven, The Netherlands) microscope equipped with a EDAX DX-4i energy dispersive X-ray analyzer with ECON IV detector (Mahwah, NJ, USA) was used. Surface structure and stomatal densities were evaluated on SEM micrographs of intact samara sections corresponding to the wing and seed regions of the two samara sides ($n = 10$ per species).

Green and dry intact samaras, and previously rehydrated dry samaras were analyzed by transmission electron microscopy (TEM). Dry samaras were rehydrated by immersion in distilled water for 8 h. Samaras were cut into 4 mm^2 pieces and fixed in 2.5% glutaraldehyde–4% paraformaldehyde (both reactants from Electron Microscopy Sciences (EMS), Hatfield, USA) for 6 h at 4 °C. Thereafter they were rinsed in ice-cold phosphate buffer (pH 7.2) four times within a period of 6 h, and left overnight in darkness at room temperature (18–20 °C). Tissues were post-fixed in a 1:1 2% aqueous OsO_4 (TAAB Laboratories, Berkshire, UK) and 3% aqueous $K_4Fe(^{13}CN)_6 \cdot 3\,H_2O$ (Sigma-Aldrich) solution for 1.5 h. Thereafter they were washed with distilled water (×3), dehydrated in a graded series of 30%, 50%, 70%, 80%, 90%, 95% and 100% acetone (two repetitions, 15 min each concentration) and embedded in acetone-Spurr's resin (TAAB Laboratories) solutions (3:1, 2 h; 1:1; 2 h; 1:3; 3 h (v:v)) and then in pure resin overnight at room temperature (25 °C). Final embedding was done in blocks, which were incubated at 70 °C for 3 days for complete polymerization. Ultrathin sections were cut, mounted on nickel grids and post-stained with Reynolds lead citrate (EMS) for 5 min. Samples were observed with a Jeol 1010 electron microscope (Tokyo, Japan) operated at 80 kV, equipped with a CCD megaview camera.

The thickness of the cuticle and external cell wall of ordinary epidermal cells of both species and the length of *U. laevis* cuticle (effective vs projected) were measured on TEM micrographs of green samaras using siViewer (Olympus Soft Imaging Solutions GmbH, Münster, Germany) and ImageJ 1.45 s (National Institutes of Health, Bethesda, MD, USA) softwares. Measurements were carried out at periclinal areas, excluding those located close to anticlinal regions ($n = 15$, 10–20 repetitions).

Samara water exchange and net photosynthetic CO_2 uptake

For both species, the water loss rates and absorption capacity were evaluated in detached green and dry samaras, respectively. The surface evaporation rate (E) of the samaras ($n = 10$) was measured gravimetrically over 20 min. The time response of further samara water losses was evaluated by recording weight variations for 4 days at room conditions (19–21°C, 34–38% RH) and fitting the values to an exponential growth to maximum function:

$$f(t) = a \times (1 - e^{-1/b \times t})$$

where a and b represent the initial water content of green samaras and the time constant, respectively (Zwieniecki et al. 2007). To facilitate interpretations, the time course of samara water loss was represented using a simple exponential decay function.

For water absorption measurements, samaras ($n = 4$ per species comprising 10 samaras each) were maintained in darkness in a closed container for 4 days at ~95% RH, a condition achieved by air exposure to a supersaturated solution of $Pb(NO_3)_2$ at 20 °C (Winston and Bates 1960). Other groups of samaras ($n = 10$ per species) were kept in a container with distilled water, and they were frequently pushed carefully to the bottom of the container. Samples were weighed at the beginning of the experimental periods and each 24 h afterwards.

Air conditions during measurements were recorded using a Hobo H21-002 Micro Station with a S-THB-M002 Temperature/RH Sensor (Onset Computer, Cape Cod, MA, USA). The RH values measured are consistent with those occurring in the natural environment of both species when samaras are on the trees (confirmed by MAGRAMA meteorological data; Venturas et al. 2013).

Net photosynthetic CO_2 uptake rate (P_n) was measured with a portable photosynthesis system (LI-6400, Li-Cor Inc., NE, USA). Measurements were conducted in situ in attached, green samaras ($n = 9$ per species) well-exposed to sunlight at ambient air temperature and RH. Irradiance was set to match ambient values, at 1500 μmol m^{-2} s^{-1}, using the LI-6400-40 blue-red light source. Air flow during measurements was set at 200 μmol s^{-1} and air CO_2 concentration at 400 ppm, using the built-in CO_2 mixer. Measurements were made at full samara expansion and so on different days for *U. minor* and *U. laevis*. Air temperature was 18.3 ± 0.7 and 23.4 ± 0.5 °C, and air vapor pressure deficit 0.77 ± 0.10 and 1.00 ± 0.20 kPa for *U. minor* and *U. laevis*, respectively. The 2 cm^2 surface area of the measurement cuvette was filled. However, in the case of *U. laevis*, whose samaras are smaller than those of *U. minor*, we placed two samaras into the cuvette to maximize CO_2 flux from plant material and minimize leakage. In addition, data were corrected to take into account diffusion leaks, as modeled by Rodeghiero et al. (2007).

The occurrence of numerous epidermal folds and a network of overlapped trichomes on samara edges in *U. laevis* lead to substantial differences between effective and projected surface areas. Therefore, and similar to samara soluble lipid amount, water loss rates and P_n were normalized by tissue DW. To facilitate comparisons, stomatal density and P_n were expressed on a projected surface area basis. Dry weight was obtained from oven-dried samaras (at 7 °C) for 3 days. The projected surface area of the samaras was calculated by analyzing scanned material with ImageJ 1.45 s and WinFOLIA (Regent Instruments Inc., Québec City, Canada) softwares. The ratio of weight to projected surface area was additionally calculated.

Samara floatability and sustentation

Two experiments were performed to determine potential differences in floatability and sustentation of *U. laevis* and *U. minor* dry samaras. For the floatability trial, samaras ($n = 20$ per species) were dropped on the water surface of two plastic containers (30 × 20 × 20 cm^3) filled with tap water (3–5 cm deep) and covered with a lid. Still and running water treatments were applied to simulate a stationary and turbulent water regime, respectively. The still water container was placed on a shelf of the laboratory, whereas the running water container was placed on an agitator set at 75 rpm creating waves that covered the samaras. During 8 days, the number of samaras that remained floating on the surface was counted every 24 h. During this time, air temperatures oscillated between 22 °C and 24 °C.

For the sustentation experiment, samaras ($n = 30$ per species) were dropped from a height of 5.36 m to measure the time that each samara took to reach the floor, and the distance at which the samara landed from the vertical drop axis. The experiment was performed in a closed warehouse, at 21 °C air temperature and with still air. The weight and projected surface area of each samara were measured.

Statistical analysis

Analysis of variance and Duncan's Multiple Range tests, and unpaired *t*-tests were undertaken using SPSS 15.0.1 statistical package (SPSS Inc., Chicago, IL, USA) to compare mean values between species and samara type (5% significance). Samara water absorption was analyzed using Student's *t*-test paired sample comparisons.

Results

Samara morphology and surface structure

Samaras of *U. laevis* had lower projected surface area and DW values as compared with *U. minor* (Table 1, Figure 1). For both species, the surface roughness of green samaras was chiefly conferred by the vascular bundles (Figure 2A and B), epidermal cells (Figure 2C and D), and epicuticular wax plates (data not shown). Conspicuous nano-folds were additionally present in *U. laevis* (Figure 2C). Stomata were often localized over the bundles, some pores being partially or fully covered with organic material (possibly waxes), especially in *U. minor* (Figure 2D). Stomatal density was approximately three times higher for *U. laevis* than *U. minor*

Table 1. Dry weight (DW), projected surface area (*A*), stomatal density, cuticle and outer cell wall thickness, soluble lipid amount, surface evaporation rate (*E*) and CO_2 assimilation rate (P_n) of *U. laevis* and *U. minor* green samaras.

Parameter	*U. laevis*	*U. minor*
DW (mg $samara^{-1}$)	3.76 ± 0.39a	12.08 ± 1.45b
A (cm^2 samara $side^{-1}$)	1.08 ± 0.06a	4.20 ± 0.38b
Stomatal density (stomata mm^{-2})	13.7 ± 2.8a	4.6 ± 1.6b
Cuticle thickness (nm)	295 ± 32	105 ± 19
Outer cell wall thickness (μm)	1.3 ± 0.2– 2.0 ± 0.2[1]	1.0 ± 0.2
Soluble lipid amount (mg g^{-1})	55.3 ± 1.8	75.9 ± 4.9
E 0–7 min (μmol g^{-1} s^{-1})	14.89 ± 5.77a	2.77 ± 1.24b
E 7–20 min (μmol g^{-1} s^{-1})	3.37 ± 1.98a	2.65 ± 0.49a
Area-based P_n (μmol m^{-2} s^{-1})	1.65 ± 0.79a	1.07 ± 0.33a
Mass-based P_n (nmol g^{-1} s^{-1})	46.8 ± 22.3a	47.5 ± 14.5a
Water loss time constant (h)	20.4 ± 2.5a	31.0 ± 6.5b

Data are means ± SD. The number of samples per species used for calculations was: 59 for DW and *A*, 10 for stomatal density, 15 for cuticle and cell wall thickness, 10 for *E* rate and water loss time constant, and 9 for P_n; 60 *U. laevis* and 40 *U. minor* were used for soluble lipid amount. Within rows, values marked with different letters are significantly different according to Duncan's Multiple Range or *t*-test ($P \leq 0.05$).
[1]Flat–convex cell wall regions.

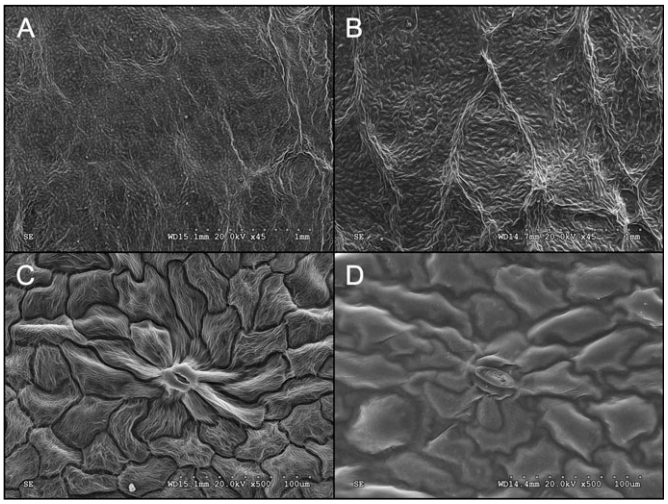

Figure 2. SEM micrographs of intact green samaras of *U. laevis* (A, C) and *U. minor* (B, D).

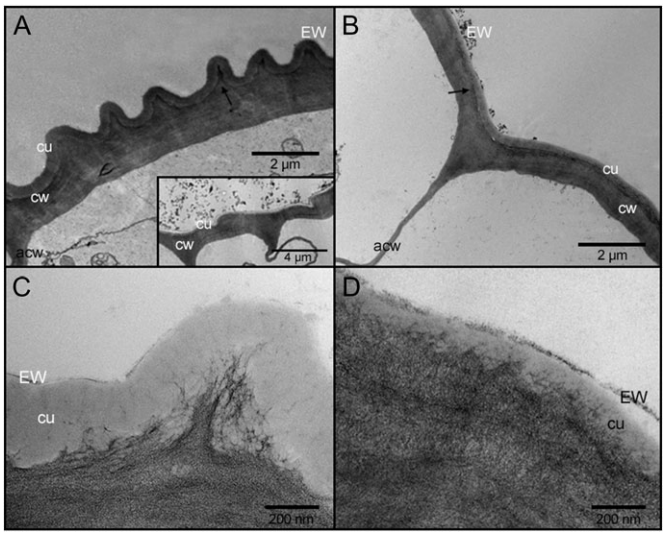

Figure 3. TEM micrographs of the outer epidermal cell wall of *U. laevis* (A, C) and *U. minor* (B, D) intact samaras. The micrographs correspond to green samaras with the exception of that in the inset box in (A), which is of a dry samara. Arrows indicate highly electron-dense material. acw, anticlinal cell wall; cw, cell wall; cu, cuticle; EW, epicuticular waxes.

(Table 1). The trichomes found along *U. laevis* samara margin were observed to be non-glandular. By contrast, *U. minor* had few glandular trichomes sparsely distributed on the wing surface (data not shown). Structural differences between the external surface of non-seed vs seed regions or samara sides were negligible.

The outer epidermal cell wall of *U. laevis* green samaras as observed by TEM was sinuous, with thicker areas giving rise to convexities that correspond to the mentioned folds (Figure 3A vs Figure 2C). These cell wall folds increased the surface area of green samaras by an approximate factor of 2.6 relative to a flat surface. The external cell wall of *U. minor* epidermis was rather smooth (Figure 3B). Highly electron-dense material was present at variable intervals in cell wall areas underneath the cuticle of the two species, including *U. laevis* folds (Figure 3A and B). According to Holloway's nomenclature (1982), the samara cuticle of both species had a 'reticulated' morphology. The 'reticulum', which was more conspicuous in *U. minor* cuticle, could sometimes be observed up to the epicuticular wax layer (Figure 3C and D). The cuticle of *U. laevis* green samaras was about three times thicker than that of *U. minor* (excluding the epicuticular wax layer), and as much as twofold higher in the case of the whole outer epidermal cell wall (Table 1).

While SEM micrographs of dry samaras showed an increased nerve protrusion for both species and tissue folding in the case of *U. minor* relative to green samaras, *U. laevis* dry samara cross-sections revealed a smoother outer epidermal wall (Figure 3A and inset box). After samara rehydration, *U. laevis* outermost cell wall regions adopted a similar aspect to green samaras (data not shown).

Chemical composition of samara surfaces

The amount of chloroform-soluble lipids was higher for *U. minor* than *U. laevis*, mean values being, respectively for each species, 75.9 vs 55.3 mg g^{-1} (green samaras), and 39.0 vs 17.2 mg g^{-1} (dry samaras). The most abundant soluble lipids identified in green samaras were long-chain primary alcohols (78.6% for *U. laevis* vs 92.4% for *U. minor*) and triterpenoids (10.1% vs 5.6%).

Scanning electron microscopy coupled to X-ray analyses revealed the presence of relatively high concentrations of silicon in the samaras, especially in *U. laevis* trichomes and as silicon bodies or aggregates randomly distributed in *U. minor* wing surface.

Qualitative information about samara chemical composition was also gained by digestion of intact (untreated) and chloroform-extracted samaras in enzymatic solutions. For both species, the application of pectinase and of cellulase plus pectinase solutions hydrolyzed samara tissues earlier than cellulase solution, especially after soluble lipid extraction. The samara cuticle of *U. laevis* could be enzymatically isolated as an intact layer having the same surface area as the samara, whereas small tissue pieces were obtained for *U. minor* after enzymatic treatments.

Ulmus laevis trichome and cuticle morphology were differently affected by the various digestion procedures (Figure 4). After short immersion of intact samaras in cellulase solution, the trichomes became fused by non-hydrolyzed material (Figure 4A), but not after the pectinase treatments (Figure 4B). A similar phenomenon could be noticed for *U. laevis* cuticle. A kind of amorphous, blurred patina was observed in the inner side of the cuticles isolated with cellulase, which was especially noticeable after soluble lipid extraction (Figure 4C and inset box). In contrast, the pectinase solutions seemed to hydrolyze the material contained between the so-called cell wall folds as observed in cuticle inner

sides (Figure 4B and inset box). The partial tissue digestion led to the observation of the venation pattern in *U. laevis* samaras, which had a thicker vascular bundle along the margin than those coming from wing inner regions (e.g., Figure 4B). In addition, *U. laevis* trichomes and some ordinary epidermal cells were found to be physically connected to samara internal tissues (Figure 4B, inset box).

Wettability and physico-chemical parameters

The contact angles (θ) of drops of water (w), glycerol (g) and diiodomethane (d) deposited onto green and dry *U. laevis* and *U. minor* samara wing surfaces are shown in Table 2. *Ulmus laevis* exhibited higher θ values, i.e., lower wettability, for the three liquids than *U. minor*. For the two species, green surfaces showed similar θ_w and θ_g, and lower θ_d. The θ_w was the highest for dry samaras. Comparing dry and green samaras, θ_w was higher in dry samaras of both species, while θ_g and θ_d were higher in dry than green samaras only for *U. minor*. No significant differences were found between samara sides. Drops of all the liquids remained attached to the surfaces when tilted and even when placed face down, indicating a high adherence of the drops to green and dry samara surfaces.

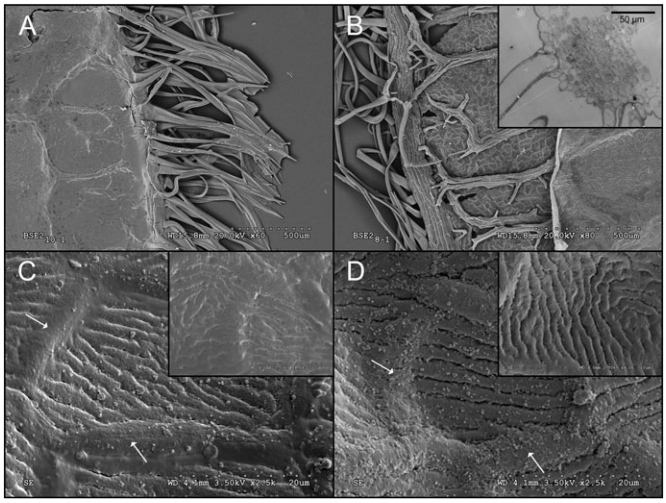

Figure 4. SEM and TEM micrographs of *U. laevis* samaras after cellulase (A, C) and pectinase (B – main box, D) hydrolysis. (A, B) Effect of 1-day (A) and 2-day (B) digestion periods on intact samaras. (B inset box) Detail of an intact samara showing the epidermal cells and subjacent tissues. (C, D) Inner side of isolated cuticles of intact (main boxes) and chloroform-extracted (inset boxes, ×4.0 k) samaras after 1-month digestion periods. Arrows indicate anticlinal cell walls.

Table 2. Contact angles of water (θ_w), glycerol (θ_g) and diiodomethane (θ_d) with the wing surface of green and dry samaras of *U. laevis* and *U. minor*.

Sample	θ_w (°)	θ_g (°)	θ_d (°)
Green *U. laevis*	121.7 ± 1.9Aa	114.3 ± 6.7Aa	79.5 ± 6.9Aa
Green *U. minor*	108.7 ± 4.9Ba	100.4 ± 5.8Ba	58.4 ± 5.9Ba
Dry *U. laevis*	135.9 ± 3.9Ab	126.1 ± 5.2Aa	80.8 ± 5.6Aa
Dry *U. minor*	123.0 ± 5.3Bb	111.5 ± 3.5Bb	70.8 ± 3.3Bb

Data are means ± SD; $n = 30$. Within columns, values marked with different letters are significantly different for species (A, B) and stage (green vs dry; a, b) according to Duncan's Multiple Range test ($P \leq 0.05$).

Table 3 shows the total surface free energy (γ_s) and its components (γ_s^{LW} and γ_s^{AB}), polarity and solubility parameter (δ) of the samara surfaces. All surfaces had a significantly high dispersive component (γ_s^{LW}) contribution as compared with the lower acid–base or non-dispersive component (γ_s^{AB}). The highest γ_s values were found for *U. minor* samara surfaces, especially for green samaras. Surface polarity approximately ranged between 16% and 17%, for green samaras and between 4% and 3.5% for dry samaras of both species. Therefore, dry samara surfaces had a lower polarity and γ_s^{AB} component compared with green, hydrated tissues. The highest δ was obtained for *U. minor* green samara surfaces (17.2 $MJ^{1/2}\,m^{-3/2}$), the remaining surfaces having values between 10.7 and 13.0 $MJ^{1/2}\,m^{-3/2}$.

Samara water exchange and net photosynthetic CO_2 uptake

The water content of readily detached green samaras was similar for both species, attaining values of 5.31 ± 0.34 g g^{-1} (*U. laevis*) and 5.34 ± 0.46 g g^{-1} (*U. minor*). The average *E* of *U. laevis* samaras at ~36% RH was more than five times higher than that of *U. minor* over the first 7 min after removing the samara from the branch. Then, *U. laevis E* experienced a substantial decrease (7–20 min) and became similar to the *E* of *U. minor*, which remained constant over the 20-min measurement period (Table 1). In general, *U. laevis* lost water more rapidly than *U. minor* at this RH, as derived from the time constant values estimated and water losses recorded for 4 days (Table 1, Figure 5). For both species, the exponential function fitted water loss data with adjusted R^2 values ranging between 0.9951 and 0.9997. Mean values of P_n were positive, and did not differ significantly between species, either expressed on a samara DW or projected area basis (Table 1).

The increment in water content after 24 h of keeping samaras at ~95% RH was slightly higher for *U. laevis* than *U. minor* (0.53 ± 0.01 vs 0.45 ± 0.01 g g^{-1}). At that time, samaras had attained their maximum hydration capacity under the experimental conditions tested. By contrast, *U. laevis* samaras increased their water content between two and four times less than

Table 3. Surface free energy per unit area (γ_s) with the corresponding Lifshitz van der Waals (γ_s^{LW}) and acid–base (γ_s^{AB}) components, polarity and total solubility parameter (δ) of the wing surface of green and dry samaras of *U. laevis* and *U. minor*.

Sample	γ_s^{LW} (mJ m^{-2})	γ_s^{AB} (mJ m^{-2})	γ_s (mJ m^{-2})	Polarity (%)	δ ($MJ^{1/2}\,m^{-3/2}$)
Green *U. laevis*	16.8	3.3	20.1	16.2	11.8
Green *U. minor*	27.6	5.7	33.3	17.2	17.2
Dry *U. laevis*	16.9	0.7	17.7	4.1	10.7
Dry *U. minor*	22.1	0.8	22.9	3.5	13.0

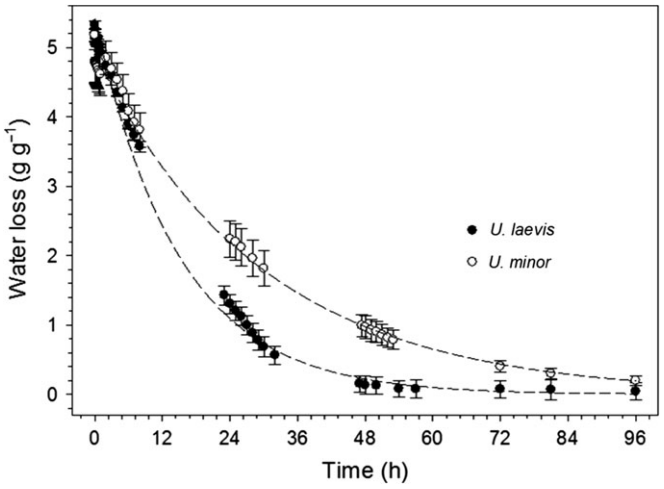

Figure 5. Time course of water loss in green samaras of *U. laevis* and *U. minor* at ~36% RH. Water losses, given as means and standard errors, are relative to samara DW. Ten samples per species were used. The experimental data have been fit with a single exponential decay function (dashed lines).

U. minor after 24 h in contact with liquid water (2.75 ± 0.15 vs 7.86 ± 2.58 g g^{-1}). It must be considered that these values were likely to be affected by an undetermined loss of water-soluble compounds.

Dispersal characteristics: samara floatability and sustentation

Differences in floatability of *U. laevis* and *U. minor* dry samaras were found when dropping samaras in the simulated turbulent water regime. After 24 h, all *U. minor* samaras sunk, whereas at that time only one *U. laevis* samara had sunk. The remaining *U. laevis* samaras gradually sunk over 8 days. In contrast, all samaras of both species dropped in still water remained floating on the surface after 8 days. It is worth noting that for both water movement regimes some *U. minor* samaras started germinating after 72 h. When the experiment ended, all *U. minor* samaras had germinated whereas none of *U. laevis* germinated.

Concerning air sustentation, the time samaras took to land on the ground was significantly different between species. Samaras of *U. minor* took longer to reach the floor (6.37 ± 0.87 s) than those of *U. laevis* (5.52 ± 1.09 s). The ratio of weight to projected surface area for *U. minor* and *U. laevis* was 4.4 ± 0.6 and 6.6 ± 2.4 mg cm^{-2}, respectively. Time and weight to surface area ratios were significantly correlated ($r = -0.8542$). No significant differences between species were found concerning the distance from the vertical axis at which the samaras landed.

Discussion

In this study we examined the surface physico-chemical and physiological features of *U. laevis* and *U. minor* samaras, as they may reflect adaptive strategies for successful seed development and dispersal and further seedling establishment. To the best of our knowledge, elm samara surface properties and water relations have not been analyzed before, and only Li et al. (2012) have studied the photosynthetic characteristics of *Ulmus pumila* samaras.

Photosynthetic capacity of elm samaras

The average P_n value expressed on a projected surface area basis was 1.65 and 1.07 μmol m^{-2} s^{-1} for *U. laevis* and *U. minor*, respectively, which is higher than the values reported for the samaras of other species. Kenzo et al. (2003) reported average P_n in dipterocarp samaras that ranged from 0.26 to −1.10 μmol m^{-2} s^{-1}. Values for *U. laevis* and *U. minor* were positive even if samaras were full and seeds likely actively respiring. Samara P_n was ~10% of light-saturated area-based P_n leaf values, and 25% mass-based P_n leaf values (Li et al. 2015). By measuring chlorophyll *a* fluorescence, Li et al. (2012) observed that potential quantum yield of photosystem II was comparable in samaras and leaves of *U. pumila*. High photochemical efficiency and potential for CO_2 assimilation have been described for other fruits (Aschan and Pfanz 2003), suggesting that low P_n of samaras might be influenced by low stomatal densities and carboxylation rates. In addition, the occlusion of stomatal pores by lipids, as sometimes observed for the samaras of the two species, and particularly *U. minor*, has been described to influence leaf CO_2 exchange and water loss to a different extent among studies (Jeffree et al. 1971, Brodribb and Hill 1997, Feild et al. 1998, Mohammadian et al. 2007, Peguero-Pina et al. 2016). Higher density of open pores in samaras of *U. laevis* than *U. minor* could contribute to (non-significantly) higher P_n per unit projected area in the former species ($P = 0.073$). Moreover, higher samara mass per unit projected area in *U. laevis* could reflect a higher volume of photosynthesizing cells, and so contribute to higher P_n on a projected area basis in this species than *U. minor*, similar to the way leaf thickness controls area-based leaf P_n across species (e.g., Niinemets 1999). The positive CO_2 assimilation rates recorded for *U. laevis* and *U. minor* samaras suggest that these fruits may contribute to seed growth and, ultimately, to tree carbon economy, as suggested for other species (Ashton 1989, Peck and Lersten 1991, Li et al. 2015). However, further studies are needed to elucidate interspecific differences in samara P_n and the consequences for tree carbon economy.

Epidermal water flux and hydration of elm samaras

The factors that influence samara water loss may also affect their water absorption. We must, however, consider the potential effect of vapor vs liquid water, and the different water sorption and desorption rates of the cuticle (Reina et al. 2001), which may additionally vary for other epidermal cell wall regions. The existence of a thicker cuticle in *U. laevis* samaras does not imply a higher or lower resistance to water loss as previously noted

(Norris 1974, Riederer and Schreiber 2001, Fernández et al. 2008). Other epidermal features such as the ratio of effective to projected surface area (higher in *U. laevis*) or the type and relative amount and distribution of e.g., pectins or soluble lipids in the cuticle and other cell wall regions may, however, affect water fluxes across the epidermis of both species. In this regard, the higher *E* values of *U. laevis* recorded for the first 7-min phase suggest the presence of substantial amounts of water close to samara evaporation sites, possibly within pectin-based gels (White et al. 2014, Figures 3A, and 4A and C). In contrast, *U. minor* had lower *E* since the beginning (until nearly full dehydration) and higher abundance of soluble cuticular lipids, which have been associated with limiting water loss (Schönherr 1976, Leide et al. 2007).

The enzymatic digestion of *U. laevis* samaras allowed us to identify the presence of pectins in the inner cuticle surface, as also derived from TEM microscopic observations. Moreover, the effect of cellulase digestion on the cuticle and trichomes of this species (Figure 4A and C) may be associated with the cross-linking of shallow, water-insoluble pectins with other cuticular chemical constituents (chiefly those remaining after chloroform extraction in the case of cuticles). This may provide evidence for the interaction between pectins and cutin monomers, and other lipidic cuticle constituents as recently described by Guzman-Puyol et al. (2015). These authors suggest a role of cell wall polysaccharides in the process of cutin biosynthesis and provided in vitro evidence for the chemical interactions between pectins and cutin monomers. However, other non-lipidic cuticle compounds may also be involved in such cross-links (e.g., mineral elements, Guzmán-Delgado et al. 2016).

The isolation of *U. laevis* cuticles and of *U. minor* small epidermal pieces after the prolonged enzymatic digestion process to which samaras were subjected reflects differences in the permeability to liquid water of the cuticles and neighboring cell wall regions between the two species (Guzmán et al. 2014*a*). Moreover, the arrangement of chemical constituents of *U. laevis* outermost cell wall regions (including the cuticle; Fernández et al. 2016) varied with tissue hydration stage, as derived from the recovery of cell wall folds after samara rehydration (Figure 3A). The potential interaction of water with pectins and the subsequent pectin hydration and expansion process may be associated with this variation, as revealed by nuclear magnetic resonance studies performed with onion and *Arabidopsis thaliana* cell walls (Ha et al. 1997, White et al. 2014). Nevertheless, an improved knowledge on cuticle structure, chemical composition and their relationship is needed to interpret such differences (Fernández et al. 2016).

Samaras of both species absorbed water through the epidermis even under non-saturated vapor conditions (~95% RH) with *U. laevis* attaining a slightly higher absorption capacity. *Ulmus laevis* trichomes, which may contain significant amounts of pectins, could constitute an uptake pathway for water, as suggested for other species and organs (e.g., Reyes-García et al. 2012, Fernández et al. 2014*b*, Pina et al. 2016). Trichomes were additionally found to be physically connected to vascular bundles, either directly or by means of mesophyll cells, which may allow fast water exchange between these tissues (Zwieniecki et al. 2007). This will contribute to samara hydration and dehydration and to their development and dispersal, respectively.

Physico-chemical properties of samara surfaces and liquid water interactions

Most studies performed during the last decades on plant surface–liquid interactions focused on the influence of surface morphology, as well as on the functionality of water repellence with only limited emphasis on chemical features (e.g., Brewer and Nuñez 2007, Rosado and Holder 2013). The low vs high degree of wettability of samara surfaces for the mainly polar (water and glycerol) vs apolar (diiodomethane) liquids, along with droplet adherence, may suggest that chemical interactions between the liquids and microscopic surface areas having contrasting properties occur. The influence of air bubbles as an additional fluid phase at the samara surface–liquid interface on samara wettability and adherence must be also considered. The solubility parameter (δ) of *U. minor* green samara surface is in the range of that of model epicuticular waxes (between 16 and 17 $MJ^{1/2}\,m^{-3/2}$, Khayet and Fernández 2012), which reflects the influence of wax chemical composition on liquid behavior. An increased roughness may lead to low δ (Khayet and Fernández 2012, Fernández et al. 2014*b*, Fernández and Khayet 2015), as it could be reckoned for dry samaras of *U. minor* and for green and dry samaras of *U. laevis* (Table 3). A similar phenomenon was observed for the total surface free energy (γ_s), which was mainly influenced by the dispersive component. In this regard, *U. laevis* cell wall nano-folds increased surface roughness and contribute to reduce the wettability (Koch and Barthlott 2009), δ and γ_s values of this species as compared with *U. minor*. The lower polarity of dry samara surfaces indicates a significantly low degree of potential polar and hydrogen-bonding interactions as compared with green samaras. Such surface features may be beneficial, for instance to prevent the immediate water absorption by the seed, thus facilitating longer dispersal distances.

Ecophysiological implications

The structural and chemical features of *U. laevis* and *U. minor* samara surfaces and the physiological parameters reported in this study can provide information on the significance of reproductive organs in relation to environmental interactions, and eventually on species ecology. The functionality of low surface wettability and high water adhesion has been addressed in few studies chiefly performed with pubescent leaves (Brewer et al. 1991, Brewer and Smith 1994, 1997), with the basis for this phenomenon remaining unclear so far (Teisala et al. 2011). Fewer studies have focused on fruit surfaces, and this is one of few attempts to link surface–water interactions to fruit and seed ecological processes (see also Fernández et al. 2011).

The adherence of water to the surface of the samaras will allow the deposition and retention of atmospheric water (e.g., rain, fog, dew). This phenomenon may facilitate the hydration of the samaras via the epidermis and, as suggested for other low-wettable plant surfaces, may reduce plant transpiration (Ritter et al. 2009), while increasing photosynthetic rates (Smith and McClean 1989, Hanba et al. 2004, Simonin et al. 2009, Urrego-Pereira et al. 2013). By contrast, Brewer and Smith (1994) found a decrease in the photosynthesis and yield of soybeans after artificial misting, which may be associated with the specific degrees of leaf wettability and water adhesion of the plants analyzed. The roughness and specific chemical composition of samara surfaces may limit the interference of surface deposited water with vapor fluxes across the epidermis; this can be particularly the case for *U. laevis* cell wall folds, which may entrap water drops, thus not impeding CO_2 fluxes across stomatal pores. Nonetheless, the relationship between plant surface physico-chemistry, liquid interactions and matter exchange deserves further studies.

The photosynthetic and epidermal water absorption capacity of the samaras, along with the potential improvement of samara and tree physiological status as influenced by samara surface–water interactions, may be of greater importance in the case of *U. minor* due to the late appearance of leaf canopy. The cuticle of *U. minor* has a relatively high abundance of soluble waxes. Without the presence of leaves, this may be interpreted as a faster and more metabolically cost-effective strategy for protection against abiotic stresses such as desiccation or excessive irradiance, in contrast to developing the more complex cuticle intuited for *U. laevis* (Fernández et al. 2014*a*), whose samaras develop at the same time as leaves. Differences between the two species in water loss rates may reflect the less conservative water-use character of *U. laevis* than *U. minor*, which is in line with the higher drought tolerance of *U. minor* and each species niche. Future works evaluating xylem water potential and non-structural carbohydrates, together with samara biomass per tree and seasonality in water and CO_2 exchange, will help to assess the importance of samara water and carbon exchange for tree performance.

The decrease in wettability and polarity of dry samara surfaces relative to green surfaces may reduce water absorption rates and hence contribute to samara dispersal until reaching suitable conditions for germination. The lower wettability of *U. laevis* samaras as compared with *U. minor* is consistent with their higher floatability and may reflect an adaptation to hydrochory. The wing roughness and especially the trichomes of *U. laevis* samara margin may function not only to enhance atmospheric water absorption, but also to promote samara floatability, even on turbulent water regimes. The trichomes might generate a significant upward force through surface tension when in contact with liquid water, as proposed for the trichome-fringed corollas of *Nymphoides* flowers, this interaction being interpreted as an adaptation to an aquatic environment (Armstrong 2002). Moreover, in a similar way to the hair on willow fruits (Seiwa et al. 2008), *U. laevis* trichomes may also contribute to a directed dispersal facilitating seed deposition in adequate niches for their germination. Samaras of *U. laevis* showed higher ratio of weight to projected surface area and weight increment under high RH conditions, which may facilitate the landing of the samaras close to the mother tree, where chances of reaching a water lamina may increase due to the species' tendency to grow in riverbeds. By contrast, the lower values recorded for *U. minor* may favor longer wind dispersal distances, and enable the samaras to reach adequate regeneration sites within the floodplain. These results are also consistent with a greater air sustentation of *U. minor* than *U. laevis* samaras, and with a faster germination when samaras are in contact with liquid water.

In conclusion, the capacity of *U. laevis* and *U. minor* samaras to assimilate CO_2 and absorb water through the epidermis, which is potentially enhanced by specific surface properties, may contribute to their self-maintenance. The surface properties of the samaras may additionally facilitate seed dispersal preferentially by water for *U. laevis* and air for *U. minor*, and so the colonization of suitable niches for the species. Further studies with samaras at selected developmental stages will be required to better understand the functional significance of these fruits as a model of photosynthetic and reproductive plant organs, and the reproductive biology and ecology of elms.

Acknowledgments

The authors are grateful to Salustiano Iglesias and David León (Spanish Ministry of Agriculture, Food and Environment, MAGRAMA) and officials from MAGRAMA for the maintenance of the Spanish Elm Breeding Program, to Jorge Domínguez (Tragsa) for his support on material collection and field measurements, and to Ramiro Martínez (Novozymes) for providing free enzyme samples.

Conflict of interest

None declared.

Funding

This work was supported by the Spanish Ministry of Economy and Competitiveness (MINECO, Project AGL2012-35580). P.G.-D. is currently supported by a 'Emilio González Esparcia' scholarship. J.R.-C. is currently supported by a 'Ramón y Cajal' contract (MINECO) co-financed by the European Social Fund.

References

Andolfillo T, di Bisceglie P, Urso T (2002) Minimum cuticular conductance and cuticle features of *Picea abies* and *Pinus cembra* needles along an altitudinal gradient in the Dolomites (NE Italian Alps). Tree Physiol 22:479–487.

Armstrong JE (2002) Fringe Science: are the corollas of *Nymphoides* (Menyanthaceae) flowers adapted for surface tension interactions? Am J Bot 89:362–365.

Aryal B, Neuner G (2010) Leaf wettability decreases along an extreme altitudinal gradient. Oecologia 162:1–9.

Aschan G, Pfanz H (2003) Non-foliar photosynthesis – a strategy of additional carbon acquisition. Flora 198:81–97.

Ashton PS (1989) Dipterocarp reproductive biology. In: Lieth H, Werger MJA (eds) Tropical rain forest ecosystems. Elsevier, Amsterdam, pp 219–240.

Berry ZC, White JC, Smith WK (2014) Foliar uptake, carbon fluxes and water status are affected by the timing of daily fog in saplings from a threatened cloud forest. Tree Physiol 34:459–470.

Boucher JF, Munson AD, Bernier PY (1995) Foliar absorption of dew influences shoot water potential and root growth in *Pinus strobus* seedlings. Tree Physiol 15:819–823.

Boyer JS (2015) Turgor and the transport of CO_2 and water across the cuticle (epidermis) of leaves. J Exp Bot 66:2625–2633.

Breshears DD, McDowell NG, Goddard KL, Dayem KE, Martens SN, Meyer CW, Brown KM (2008) Foliar absorption of intercepted rainfall improves woody plant water status most during drought. Ecology 89:41–47.

Brewer CA, Nuñez CI (2007) Patterns of leaf wettability along an extreme moisture gradient in western Patagonia, Argentina. Int J Plant Sci 168:555–562.

Brewer CA, Smith WK (1994) Influence of simulated dewfall on photosynthesis and yield in soybean isolines (*Glycine max* [L.] merr. cv Williams) with different trichome densities. Int J Plant Sci 155:460–466.

Brewer CA, Smith WK (1997) Patterns of leaf surface wetness for montane and subalpine plants. Plant Cell Environ 20:1–11.

Brewer CA, Smith WK, Vogelmann TC (1991) Functional interaction between leaf trichomes, leaf wettability and the optical properties of water droplets. Plant Cell Environ 14:955–962.

Brodribb T, Hill RS (1997) Imbricacy and stomatal wax plugs reduce maximum leaf conductance in Southern Hemisphere conifers. Aust J Bot 45:657–668.

Buckley TN (2016) Stomatal responses to humidity: has the 'black box' finally been opened? Plant Cell Environ 39:482–484.

Burkhardt J, Basi S, Pariyar S, Hunsche M (2012) Stomatal penetration by aqueous solutions – an update involving leaf surface particles. New Phytol 196:774.

Damour G, Simonneau T, Cochard H, Urban L (2010) An overview of models of stomatal conductance at the leaf level. Plant Cell Environ 33: 1419–1438.

Eller CB, Lima AL, Oliveira RS (2016) Cloud forest trees with higher foliar water uptake capacity and anisohydric behavior are more vulnerable to drought and climate change. New Phytol 211:489–501.

Farquhar GD, Ehleringer JR, Hubick KT (1989) Carbon isotope discrimination and photosynthesis. Annu Rev Plant Biol 40:503–537.

Feild TS, Zwieniecki MA, Donoghue MJ, Holbrook NM (1998) Stomatal plugs of *Drimys winteri* (Winteraceae) protect leaves from mist but not drought. Proc Natl Acad Sci USA 95:14256–14259.

Fernández V, Eichert T (2009) Uptake of hydrophilic solutes through plant leaves: current state of knowledge and perspectives of foliar fertilization. Crit Rev Plant Sci 28:36–68.

Fernández V, Khayet M (2015) Evaluation of the surface free energy of plant surfaces: toward standardizing the procedure. Front Plant Sci 6:510.

Fernández V, Eichert T, del Río V, López-Casado G, Heredia-Guerrero JA, Abadía A, Heredia A, Abadía J (2008) Leaf structural changes associated with iron deficiency chlorosis in field-grown pear and peach: physiological implications. Plant Soil 311:161–172.

Fernández V, Khayet M, Montero-Prado P et al. (2011) New insights into the properties of pubescent surfaces: peach fruit as model. Plant Physiol 156:2098–2108.

Fernández V, Guzmán P, Peirce CAE, McBeath TM, Khayet M, McLaughlin MJ (2014*a*) Effect of wheat phosphorus status on leaf surface properties and permeability to foliar applied phosphorus. Plant Soil 384:7–20.

Fernández V, Sancho-Knapik D, Guzmán P et al. (2014*b*) Wettability, polarity, and water absorption of holm oak leaves: Effect of leaf side and age. Plant Physiol 166:168–180.

Fernández V, Guzmán-Delgado P, Graça J, Santos S, Gil L (2016) Cuticle structure in relation to chemical composition: re-assessing the prevailing model. Front Plant Sci 7:427.

Fowkes FM (1963) Additivity of intermolecular forces at interfaces. I. Determination of the contribution to surface and interfacial tensions of dispersion forces in various liquids. J Phys Chem 67: 2538–2541.

Goldsmith GR, Bentley LP, Shenkin A et al. (2016) Variation in leaf wettability traits along a tropical montane elevation gradient. New Phytol. doi:10.1111/nph.14121.

Gouvra E, Grammatikopoulos G (2003) Beneficial effects of direct foliar water uptake on shoot water potential of five chasmophytes. Can J Bot 81:1278–1284.

Guzmán P, Fernández V, García ML, Khayet M, Fernández A, Gil L (2014*a*) Localization of polysaccharides in isolated and intact cuticles of eucalypt, poplar and pear leaves by enzyme-gold labelling. Plant Physiol Biochem 76:1–6.

Guzmán P, Fernández V, Graça J, Cabral V, Kayali N, Khayet M, Gil L (2014*b*) Chemical and structural analysis of *Eucalyptus globulus* and *E. camaldulensis* leaf cuticles: a lipidized cell wall region. Front Plant Sci 5:481.

Guzmán-Delgado P, Graça J, Cabral V, Gil L, Fernández V (2016) The presence of cutan limits the interpretation of cuticular chemistry and structure: *Ficus elastica* leaf as an example. Physiol Plant 157: 205–220.

Guzman-Puyol S, Benítez JJ, Domínguez E, Bayer IS, Cingolani R, Athanassiou A, Heredia A, Heredia-Guerrero JA (2015) Pectin-lipid self-assembly: influence on the formation of polyhydroxy fatty acids nanoparticles. Plos One 10:e0124639.

Ha MA, Apperley DC, Jarvis MC (1997) Molecular rigidity in dry and hydrated onion cell walls. Plant Physiol 115:593–598.

Hanba YT, Moriya A, Kimura K (2004) Effect of leaf surface wetness and wettability on photosynthesis in bean and pea. Plant Cell Environ 27: 413–421.

Hancock BC, York P, Rowe RC (1997) The use of solubility parameters in pharmaceutical dosage form design. Int J Pharm 148:1–21.

Hansen CM (2004) 50 Years with solubility parameters-past and future. Prog Org Coat 51:77–84.

Hildebrand JH (1949) A critique of the theory of solubility of nonelectrolytes. Chem Rev 44:37–45.

Holloway PJ (1970) Surface factors affecting the wetting of leaves. Pestic Sci 1:156–163.

Holloway PJ (1982) Structure and histochemistry of plant cuticular membrane: an overview. In: Cutler DF, Alvin KL, Price CE (eds) The plant cuticle, Linnean Society Symposium Series Vol. 10. Academic Press, London, pp 1–32.

Jeffree CE, Johnson RPC, Jarvis PG (1971) Epicuticular wax in the stomatal antechamber of Sitka spruce and its effects on the diffusion of water vapour and carbon dioxide. Planta 98:1–10.

Kenzo T, Ichie T, Ninomiya I, Koike T (2003) Photosynthetic activity in seed wings of Dipterocarpaceae in a masting year: Does wing photosynthesis contribute to reproduction? Photosynthetica 41:551–557.

Khayet M, Fernández V (2012) Estimation of the solubility parameter of model plant surfaces and agrochemicals: a valuable tool for understanding plant surface interactions. Theor Biol Med Mod 9:45.

Khayet M, Vazquez Alvarez M, Khulbe KC, Matsuura T (2007) Preferential surface segregation of homopolymer and copolymer blend films. Surface Sci 601:885–895.

Koch K, Barthlott W (2009) Superhydrophobic and superhydrophilic plant surfaces: an inspiration for biomimetic materials. Philos Trans R Soc A 367:1487–1509.

Kwok DY, Neumann AW (1999) Contact angle measurement and contact angle interpretation. Adv Colloid Interfac 81:167–249.
Leide J, Hildebrandt U, Reussing K, Riederer M, Vogg G (2007) The developmental pattern of tomato fruit wax accumulation and its impact on cuticular transpiration barrier properties: effects of a deficiency in a β-ketoacyl-coenzyme A synthase (LeCER6). Plant Physiol 144:1667–1679.
Li L, Pan X, Li H (2012) Responses of photosystem II (PSII) function in leaves and samaras of *U. pumila* to chilling and freezing temperatures and subsequent recovery. Int J Agric Biol 14:739–744.
Li M, López R, Venturas M, Pita P, Gordaliza GG, Gil L, Rodríguez-Calcerrada J (2015) Greater resistance to flooding of seedlings of *Ulmus laevis* than *Ulmus minor* is related to the maintenance of a more positive carbon balance. Trees 29:835–848.
Mohammadian MA, Watling JR, Hill RS (2007) Do waxy stomatal plugs impact leaf gas exchange in a rain forest gymnosperm *Agathis robusta*? Gen Appl Plant Physiol 33:203–220.
Munné-Bosch S, Nogues S, Alegre L (1999) Diurnal variations of photosynthesis and dew absorption by leaves in two evergreen shrubs growing in Mediterranean field conditions. New Phytol 144:109–119.
Nathan R, Muller-Landau HC (2000) Spatial patterns of seed dispersal, their determinants and consequences for recruitment. Trends Ecol Evol 15:278–285.
Niinemets Ü (1999) Components of leaf dry mass per area – thickness and density – alter leaf photosynthetic capacity in reverse directions in woody plants. New Phytol 144:35–47.
Nilsson C, Brown RL, Jansson R, Merritt DM (2010) The role of hydrochory in structuring riparian and wetland vegetation. Biol Rev 85:837–858.
Norris RF (1974) Penetration of 2, 4-D in relation to cuticle thickness. Am J Bot 71:74–79.
Peck CJ, Lersten NR (1991) Samara development of black maple (*Acer saccharum* ssp. *nigrum*) with emphasis on the wing. Can J Bot 69: 1349–1360.
Peguero-Pina JJ, Sisó S, Fernández-Marín B, Flexas J, Galmés J, García-Plazaola JI, Niinemets Ü, Sancho-Knapik D, Gil-Pelegrín E (2016) Leaf functional plasticity decreases the water consumption without further consequences for carbon uptake in *Quercus coccifera* L. under Mediterranean conditions. Tree Physiol 36:356–367.
Perea R, Venturas M, Gil L (2013) Empty seeds are not always bad: simultaneous effect of seed emptiness and masting on animal seed predation. Plos One 8:e65573.
Pierce S, Maxwell K, Griffiths H, Winter K (2001) Hydrophobic trichome layers and epicuticular wax powders in Bromeliaceae. Am J Bot 88: 1371–1389.
Pina AL, Zandavalli RB, Oliveira RS, Martins FR, Soares AA (2016) Dew absorption by the leaf trichomes of *Combretum leprosum* in the Brazilian semiarid region. Funct Plant Biol 43:851–861.
Reina JJ, Domínguez E, Heredia A (2001) Water sorption–desorption in conifer cuticles: the role of lignin. Physiol Plant 112:372–378.
Reyes-García C, Mejia-Chang M, Griffiths H (2012) High but not dry: diverse epiphytic bromeliad adaptations to exposure within a seasonally dry tropical forest community. New Phytol 193:745–754.
Riederer M, Schreiber L (2001) Protecting against water loss: analysis of the barrier properties of plant cuticles. J Exp Bot 52:2023–2032.
Ritter A, Regalado CM, Aschan G (2009) Fog reduces transpiration in tree species of the Canarian relict heath-laurel cloud forest (Garajonay National Park, Spain). Tree Physiol 29:517–528.
Rodeghiero M, Niinemets Ü, Cescatti A (2007) Major diffusion leaks of clamp-on leaf cuvettes still unaccounted: how erroneous are the estimates of Farquhar et al. model parameters. Plant Cell Environ 30:1006–1022.
Rosado BH, Holder CD (2013) The significance of leaf water repellency in ecohydrological research: a review. Ecohydrology 6:150–161.
Schönherr J (1976) Water permeability of isolated cuticular membranes: the effect of cuticular waxes on diffusion of water. Planta 131: 159–164.
Seiwa K, Tozawa M, Ueno N, Kimura M, Yamasaki M, Maruyama K (2008) Roles of cottony hairs in directed seed dispersal in riparian willows. Plant Ecol 198:27–35.
Simonin KA, Santiago LS, Dawson TE (2009) Fog interception by *Sequoia sempervirens* (D. Don) crowns decouples physiology from soil water deficit. Plant Cell Environ 32:882–892.
Smith WK, McClean TM (1989) Adaptive relationship between leaf water repellency, stomatal distribution, and gas exchange. Am J Bot 76: 465–469.
Teisala H, Tuominen M, Kuusipalo J (2011) Adhesion mechanism of water droplets on hierarchically rough superhydrophobic rose petal surface. J Nanomater 2011:818707.
Urrego-Pereira YF, Martínez-Cob A, Fernández V, Cavero J (2013) Daytime sprinkler irrigation effects on net photosynthesis of maize and alfalfa. Agron J 105:1515–1528.
van Krevelen DW, Hoftyzer PJ (1976) Properties of polymers: their estimation and correlation with chemical structure, 2nd edn. Elsevier, Amsterdam.
van Krevelen DW, te Nijenhuis K (2009) Cohesive properties and solubility. In: van Krevelen DW, te Nijenhuis K (eds) Properties of polymers: their correlation with chemical structure; their numerical estimation and prediction from additive group contributions, 4th edn. Elsevier, Oxford, pp 189–227.
van Oss CJ, Chaudhury MK, Good RJ (1987) Monopolar surfaces. Adv Colloid Interfac 28:35–64.
van Oss CJ, Chaudhury MK, Good RJ (1988) Interfacial Lifshitz-van der Waals and polar interactions in macroscopic systems. Chem Rev 88: 927–941.
van Wittenberghe S, Adriaenssens S, Staelens J, Verheyen K, Samson R (2012) Variability of stomatal conductance, leaf anatomy, and seasonal leaf wettability of young and adult European beech leaves along a vertical canopy gradient. Trees 26:1427–1438.
Venturas M, López R, Gascó A, Gil L (2013) Hydraulic properties of European elms: xylem safety-efficiency tradeoff and species distribution in the Iberian Peninsula. Trees 27:1691–1701.
Venturas M, Fernández V, Nadal P, Guzmán P, Lucena JJ, Gil L (2014*a*) Root iron uptake efficiency of *Ulmus laevis* and *U. minor* and their distribution in soils of the Iberian Peninsula. Front Plant Sci 5:104.
Venturas M, Nanos N, Gil L (2014*b*) The reproductive ecology of *Ulmus laevis* Pallas in a transformed habitat. For Ecol Manage 312: 170–178.
Wang BC, Smith TB (2002) Closing the seed dispersal loop. Trends Ecol Evol 17:379–386.
White PB, Wang T, Park YB, Cosgrove DJ, Hong M (2014) Water-polysaccharide interactions in the primary cell wall of *Arabidopsis thaliana* from polarization transfer solid-state NMR. J Am Chem Soc 136: 10399–10409.
Wiegrefe SJ, Sytsma KJ, Guries RP (1994) Phylogeny of Elms (*Ulmus*, Ulmaceae): molecular evidence for a Sectional Classification. Syst Bot 19:590–612.
Willson MF, Traveset A (2000) The ecology of seed dispersal. In: Fenner E (ed) Seeds: the ecology of regeneration in plant communities. CABI, Oxford, pp 85–110.
Winston PW, Bates DH (1960) Saturated solutions for the control of humidity in biological research. Ecology 41:232–237.
Yeats TH, Rose JK (2013) The formation and function of plant cuticles. Plant Physiol 163:5–20.
Zwieniecki MA, Boyce CK (2014) Evolution of a unique anatomical precision in angiosperm leaf venation lifts constraints on vascular plant ecology. Proc R Soc B 281:2013–2829.
Zwieniecki MA, Brodribb TJ, Holbrook NM (2007) Hydraulic design of leaves: insights from rehydration kinetics. Plant Cell Environ 30: 910–921.